A combined mixed finite element method and local discontinuous Galerkin method for miscible displacement problem in porous media *

Hui Guo[1], Qinghua Zhang[1], Yang Yang[2]

[1] *College of Science, China University of Petroleum, Qingdao 266580, China.*
[2] *Michigan Technological University, Houghton, MI 49931, USA.*

Abstract: A combined method consisting of the mixed finite element method for flow and the local discontinuous Galerkin method for transport is introduced for the one dimensional coupled system of incompressible miscible displacement problem. Optimal error estimates in $L^\infty(0,T;L^2)$ for concentration c, in $L^2(0,T;L^2)$ for c_x and $L^\infty(0,T;L^2)$ for velocity u are derived. The main technical difficulties in the analysis include the treatment of the inter-element jump terms which arise from the discontinuous nature of the numerical method, the nonlinearity, and the coupling of the models. Numerical experiments are performed to verify the theoretical results. Finally we apply this method to the one dimensional compressible miscible displacement problem and give the numerical experiments to confirm the efficiency of the scheme.

Keywords: mixed finite element method; local discontinuous Galerkin method; error estimate; miscible displacement problem

AMS(2000) Subject Classifications: 65M15, 65M60.

1. Introduction

Numerical modeling of miscible displacement in porous media is important and interesting in oil recovery and enviromental pollution problem. The miscible displacement problem is described by a coupled system of non-linear partial differential equations. The need for accurate solutions to the coupled equations challenges numerical analysts to design new methods.

The mixed finite element methods [1], [2] gained great popularity in the last two decades for the reasons that they provide very accurate approximations of the primary unknown and its flux and they conserve mass locally. This method has been widely used in the numerical simulation for porous media problems since the early period of 1980s [3], [4]. The discontinuous Galerkin (DG) method gained even greater popularity recently

*Correspondence to: Hui Guo, College of Science, China University of Petroleum, Qingdao 266580, China (Email: sdugh@163.com)

for at least four reasons: 1) the flexibility inherent to it allows more general meshes construction and degree of nonuniformity than permitted by the more conventional finite element method; 2) it also conserves mass locally on any element; 3) it has, in general, less numerical diffusion and provides more accurate local approximations for problems with rough coefficients; 4) it is easy to implement. The DG method is a class of finite element method, using discontinuous, piecewise polynomials as both the solution and the test spaces. It was first designed to solve hyperbolic conservation laws containing only first order spatial derivatives, see Reed and Hill [5] for linear equations, and Cockburn et al. [6], [7], [8], [9] for nonlinear ones.

However, It is difficult to apply the DG method directly to the equations with higher order derivatives. The idea of the local discontinuous Galerkin (LDG) method is to rewrite the equations with higher order derivatives into a first order system, then apply the DG method on the system. The design of the numerical fluxes is the key ingredient to ensure stability. The first LDG method was constructed by Cockburn and Shu in [10] for solving nonlinear convection diffusion equations containing second order spatial derivatives. Their work was motivated by the successful numerical experiments of Bassi and Rebay [11] for the compressible Navier-Stokes equations. The methods were further developed in [12], [13], [14] for solving many nonlinear wave equations with higher order derivatives. The first a priori error estimate for the LDG method of linear convection-diffusion equations was obtained by Cockburn and Shu [10]. Later, Castillo et al. [15], [16] proved the optimal rate of convergence order $O(h^{k+1})$ for the LDG method with a particular numerical flux. Recently, Liu and Shu [17] considered drift-diffusion (DD) and high-field (HF) models of one-dimensional devices and provide the error estimate of order $O(h^{k+\frac{1}{2}})$. Xu and Shu [18] introduced a general approach for proving optimal L^2 error estimates for the semi-discrete LDG methods solving the one-dimensional third order, fifth order wave equation and the multidimensional Schrödinger equation. A priori error estimates for the fully discrete Runge-Kutta LDG methods with smooth solutions for the convection-dominated Sobolev equations [19] were presented by Zhang and Shu.

Although there have been many theoretical analysis of the LDG method, optimal error estimates for incompressible miscible displacement problem seems to be still unavailable. In this paper, a combined method consisting of the mixed finite element method for flow and the LDG method for transport is introduced for the one-dimensional coupled system of incompressible miscible displacement problem. In [20], [21], the interior penalty discontinuous Galerkin (IPDG) method was introduced. The authors give optimal error estimates in $L^2(0,T;H^1)$ for concentration c, and $L^\infty(0,T;L^2)$ for velocity u. In our work, we consider the LDG method and prove $L^\infty(0,T;L^2)$ for concentration c, in $L^2(0,T;L^2)$ for c_x and $L^\infty(0,T;L^2)$ for velocity u. Instead of the cut-off operator introduced in [20],

[21], in our proof, induction hypothesis is used as a tool, which can avoid the difficulty in how to choose the sufficiently large positive constant M, and the possibility of infinite times of loops for extreme cases. A simulation is also performed to validate the analysis. Then we apply this method to the one-dimensional compressible miscible displacement problem and demonstrate the efficiency of the scheme.

The paper is organized as follows. In Section 2, we present some preliminaries, including the norms we use throughout the paper, some essential properties of the finite element spaces, DG spatial discretization as well as the error equations. Section 3 is the main body of the paper where we present the methods and the details of the optimal error estimates for incompressible miscible displacement problem. Then numerical results are given to demonstrate the accuracy and capability of the methods. The discussions for the compressible miscible displacement problem are given in Section 4. We will end in Section 5 with some concluding remarks.

2. Preliminaries

In this section, we introduce some notations and definitions to be used later in the paper and also present some auxiliary results.

2.1. Basic notations

We assume the following mesh to cover the computational domain I, consisting of cells $I_j = [x_{j-\frac{1}{2}}, x_{j+\frac{1}{2}}]$, for $1 \le j \le n$, where

$$x_{\frac{1}{2}} < x_{\frac{3}{2}} < \cdots < x_{n+\frac{1}{2}}. \tag{2.1}$$

The cell centers are denoted by $x_j = (x_{j-\frac{1}{2}} + x_{j+\frac{1}{2}})/2$. We also set $\Delta x_j = x_{j+\frac{1}{2}} - x_{j-\frac{1}{2}}$ and $h = \max_j \Delta x_j$. We denote by $u^-_{j+\frac{1}{2}}$ and $u^+_{j+\frac{1}{2}}$ the values of u at the discontinuity point $x_{j+\frac{1}{2}}$, from left and right, respectively. The finite element space is chosen as

$$V_h^k = \{v : v|_{I_j} \in P^k(I_j), j = 1, \cdots, n\},$$

where $P^k(I_j)$ denotes polynomials of degree up to k defined on the cell I_j. Note that functions in V_h^k are discontinuous across element interfaces. This is one of the main differences between the DG method and traditional finite element methods. Moreover, both the mesh sizes Δx_j and the degree of polynomials k can be changed from element to element freely, thus allowing for easy h_p adaptivity.

Throughout this paper, the symbols K and ϵ are used as a generic constant and a generic small positive constant respectively, which may appear differently at different occurrences.

2.2. Projections and interpolation properties

In what follows, we define the standard L^2 -projection P_h and two special projections $P_h^{\pm}$ into V_h^k: for any given function $u \in H^1(I)$ and arbitrary subinterval $I_j = [x_{j-\frac{1}{2}}, x_{j+\frac{1}{2}}]$, the special projections of u, denoted by $P_h^+ u$ and $P_h^- u$, are the unique functions in the finite element space V_h^k satisfying, for each j,

$$\int_{I_j} (P_h^+ u(x) - u(x))\rho(x)dx = 0, \quad \forall \rho \in P^{k-1}(I_j), (P_h^+ u)^+_{j-\frac{1}{2}} = u(x_{j-\frac{1}{2}});$$
$$\int_{I_j} (P_h^- u(x) - u(x))\rho(x)dx = 0, \quad \forall \rho \in P^{k-1}(I_j), (P_h^- u)^-_{j+\frac{1}{2}} = u(x_{j+\frac{1}{2}}).$$

For the special projections mentioned above, we have, by the standard approximation theory [23], that

$$\|\eta\| + h\|\eta_x\| + h^{\frac{1}{2}}\|\eta\|_{\Gamma_h} \le Kh^{k+1}, \tag{2.2}$$

where $\eta = P_h u - u$ or $\eta = P_h^{\pm} u - u$. The positive constant K, solely depending on u, is independent of h. Here and below, an unmarked norm $\|\cdot\|$ is the usual L^2 norm defined on the interval I, and $\|\cdot\|_{\Gamma_h}$ denotes the L^2 norm defined on the cell interfaces of the mesh. For example, for the one-dimensional case under consideration in this paper, $\|\eta\|^2_{\Gamma_h} = \sum_{j=1}^{n}((\eta^+_{j+\frac{1}{2}})^2 + (\eta^-_{j-\frac{1}{2}})^2)$. Moreover, the Sobolevs inequality implies that

$$\|\eta\|_{0,\infty} \le Kh^{k+\frac{1}{2}}, \tag{2.3}$$

where the positive constant K is independent of h.

2.3. Inverse properties

In the proof of the error estimates the following inverse properties are needed: For any $v \in V_h^k$, there exists a positive constant K independent of v and h, such that

$$\|v_x\| \le Kh^{-1}\|v\|, \qquad \|v\|_{\Gamma_h} \le Kh^{-1/2}\|v\|, \qquad \|v\|_{0,\infty} \le Kh^{-d/2}\|v\|, \tag{2.4}$$

where d is the spatial dimension. In our case $d = 1$.

3. Incompressible miscible displacement problem

In this section, we give the analysis for incompressible miscible displacement problem. Detailed discussion on physical theories of miscible displacement in porous media can be found in [24, 25]. Let Ω be a bounded domain. The classical equations governing the one-dimensional incompressible miscible displacement in porous media are as follows.

$$u_x = -(\frac{k(x)}{\mu(c)}p_x)_x = q, \quad x \in I, \quad 0 < t \le T, \tag{3.1}$$

$$\phi(x)\frac{\partial c}{\partial t} + uc_x - (D(u)c_x)_x = (\tilde{c} - c)q, \quad x \in I, \quad 0 < t \le T, \tag{3.2}$$

where the dependent variables are p, the pressure in the fluid mixture, and u, the Darcy velocity of the mixture (volume flowing across a unit across-section per unit time), and c, the concentration of interested species measured in amount of species per unit volume of the fluid mixture. ϕ and k are the porosity and the permeability of the rock, respectively. μ is the concentration-dependent viscosity. q is the external flow rate, which is positive if fluid is being injected. Concentration $\tilde{c}$ in the source term is the injected concentration c_w if $q \geq 0$ and is the resident concentration c if $q < 0$. The diffusion coefficient D arises from two sources, molecular diffusion, which is rather small for field-scale problems, and a velocity-dependent term called dispersion in the petroleum engineering literature. Its form is

$$D = \phi(x)(d_{mol}I + d_{long}|u|E + d_{tran}|u|E^{\perp}),$$

where E represents projection along the velocity vector and is given by

$$E = (e_{ij}(u)) = (\frac{u_i u_j}{|u|^2}), u = (u_1, \cdots, u_n),$$

and $E^{\perp} = I - E$ is the complementary projection. The diffusion coefficient d_{long} measures the dispersion in the direction of the flow and d_{tran} shows that transverse to the flow. In general, assume that the tensor matrix $D(u)$ is positive definite. But in many actual problems, the matrix is only positive semi-definite. Note that the pressure is determined only up to an additive constant, thus, the conditions $\int_I p dx = 0, 0 \leq t \leq T$, can be applied to suppress the ambiguity. For simplicity, we assume the solution to be periodic in each independent variable. The initial concentration is given as

$$c(x, 0) = c_0(x), x \in I. \tag{3.3}$$

3.1. Weak form and the LDG scheme

First, the mixed finite element method is used to solve the flow equation: find $(u_h, p_h) \in W_h^{k+1} \times Z_h^k$ such that

$$\begin{cases} (\mu(c_h)k(x)^{-1}u_h, \theta) - (\theta_x, p_h) = 0, & \forall \theta \in W_h^{k+1}, \\ ((u_h)_x, \zeta) = (q, \zeta), & \forall \zeta \in Z_h^k, \end{cases} \tag{3.4}$$

where $W_h^{k+1} = \{\theta \in C^0(I) : \theta|_{I_j} \in P^{k+1}(I_j)\}, Z_h^k = \{\zeta \in L^2(I) : \zeta|_{I_j} \in P^k(I_j)\} = V_h^k$.

To construct the LDG scheme for transport equation, firstly we introduce some auxiliary variables to approximate the derivatives of the solution which further yields a first order system:

$$\phi(x)\frac{\partial c}{\partial t} + (uc)_x + z_x = \tilde{c}q, \tag{3.5}$$

$$s = -c_x, \tag{3.6}$$

$$z = D(u)s. \tag{3.7}$$

We multiply equations (3.5)-(3.7) by test functions v, w, ψ respectively, and formally integrate by parts for all terms involving a spatial derivative to get

$$\int_{I_j} \phi(x)\frac{\partial c}{\partial t}vdx - \int_{I_j} ucv_x dx + (uc)_{j+\frac{1}{2}}v^-_{j+\frac{1}{2}} - (uc)_{j-\frac{1}{2}}v^+_{j-\frac{1}{2}}$$
$$- \int_{I_j} zv_x dx + z_{j+\frac{1}{2}}v^-_{j+\frac{1}{2}} - z_{j-\frac{1}{2}}v^+_{j-\frac{1}{2}} = \int_{I_j} \tilde{c}qvdx, \tag{3.8}$$

$$\int_{I_j} swdx - \int_{I_j} cw_x dx + c_{j+\frac{1}{2}}w^-_{j+\frac{1}{2}} - c_{j-\frac{1}{2}}w^+_{j-\frac{1}{2}} = 0, \tag{3.9}$$

$$\int_{I_j} z\psi dx - \int_{I_j} D(u)s\psi dx = 0. \tag{3.10}$$

Replacing the exact solutions u, c, s and z in the above equations by their numerical approximations u_h, c_h, s_h and z_h , noticing that the numerical solutions c_h, s_h and z_h are not continuous on the cell boundaries, then replacing terms on the cell boundaries by suitable numerical fluxes, we obtain the LDG scheme:

$$\int_{I_j} \phi(x)\frac{\partial c_h}{\partial t}vdx - \int_{I_j} u_h c_h v_x dx + (\widehat{u_h c_h})_{j+\frac{1}{2}}v^-_{j+\frac{1}{2}} - (\widehat{u_h c_h})_{j-\frac{1}{2}}v^+_{j-\frac{1}{2}}$$
$$- \int_{I_j} z_h v_x dx + \widehat{z_h}_{j+\frac{1}{2}}v^-_{j+\frac{1}{2}} - \widehat{z_h}_{j-\frac{1}{2}}v^+_{j-\frac{1}{2}} = \int_{I_j} \tilde{c_h}qvdx, \tag{3.11}$$

$$\int_{I_j} s_h wdx - \int_{I_j} c_h w_x dx + \hat{c_h}_{j+\frac{1}{2}}w^-_{j+\frac{1}{2}} - \hat{c_h}_{j-\frac{1}{2}}w^+_{j-\frac{1}{2}} = 0, \tag{3.12}$$

$$\int_{I_j} z_h\psi dx - \int_{I_j} D(u_h)s_h\psi dx = 0. \tag{3.13}$$

The important thing is that $\widehat{u_h c_h}$ should be chosen based on upwinding, and $\widehat{z_h}$ and $\widehat{c_h}$ should be chosen alternatively from the left and the right. We choose $\widehat{z_h} = z_h^-, \widehat{c_h} = c_h^+$ and $\widehat{u_h c_h} = \max(u_h, 0)c_h^- + \min(u_h, 0)c_h^+$. We choose the initial condition $c_h^0 = P_h^+ c_0$, then we have

$$\|c(x,0) - c_h(x,0)\| \leq Kh^{k+1}.$$

3.2. A priori error estimates

In this section, we obtain the optimal error estimates for the approximation c_h, s_h, z_h which are given by the LDG method.

We make the following hypotheses (H) for the above problem.

I. $0 < k_* \leq k(x) \leq k^*, 0 < \mu_* \leq \mu(c) \leq \mu^*$, $\mu(c)$ is uniformly Lipschtiz continuous with respect to c.

II. $0 < \phi_* \leq \phi(x) \leq \phi^*, |q| \leq K$.

III. $0 < D_* \leq D(u) \leq D^*$, then $D(u)$ is uniformly Lipschtiz continuous with respect to u.

IV. u, u_x, c, c_x are bounded.

V. We will need a hypothesis, for small enough h,

$$\|u - u_h\| \leq h^{\frac{3}{2}}. \tag{3.14}$$

From (2.3) and (2.4), we obtain that $\|u - u_h\|_{0,\infty} = O(h), \|u_h\|_{0,\infty} \leq K$. under this assumption, We also easily proved $0 < k_1 \leq D(u_h) \leq k_2$.

Lemma 3.1 Let u, p be the exact solution of the problem (3.1), and let u_h, p_h be the numerical solution of the semi-discrete mixed finite element method (3.4), then we have

$$\|u - u_h\| \leq Kh^{k+1} + K\|c - c_h\|, \tag{3.15}$$

$$\|(u - u_h)_x\| \leq Kh^{k+1}. \tag{3.16}$$

The proof of this lemma is given in the appendix.

We introduce the DG discretization operator $\mathcal{D}$ as in [18] for each cell $I_j = [x_{j-\frac{1}{2}}, x_{j+\frac{1}{2}}]$,

$$\mathcal{D}_{I_j}(\rho, \phi; \hat{\rho}) = (\rho, \phi_x)_{I_j} - (\hat{\rho}\phi^-)_{j+\frac{1}{2}} + (\hat{\rho}\phi^+)_{j-\frac{1}{2}}. \tag{3.17}$$

We also use the notation

$$\mathcal{D}(\rho, \phi; \hat{\rho}) = \sum_j \mathcal{D}_{I_j}(\rho, \phi; \hat{\rho}). \tag{3.18}$$

Using the definition of the jump and the average of the functions and periodic boundary conditions, we can easily prove the following lemmas.

Lemma 3.2 Choosing different numerical fluxes, the DG discretization operator satisfies the following equalities:

$$\mathcal{D}(\rho, \phi; \rho^-) + \mathcal{D}(\phi, \rho; \phi^+) = 0, \qquad \mathcal{D}(\rho, \phi; \rho^+) + \mathcal{D}(\phi, \rho; \phi^-) = 0. \tag{3.19}$$

Lemma 3.3 For any $\phi \in V_h^k$, we have

$$\mathcal{D}(\rho - P_h^- \rho, \phi; (\rho - P_h^- \rho)^-) = 0, \qquad \mathcal{D}(\rho - P_h^+ \rho, \phi; (\rho - P_h^+ \rho)^+) = 0, \tag{3.20}$$

where P_h^+, P_h^- are the projections defined in section 2.2.

Theorem 3.1 Let c, s, z be the exact solution of the problem (3.5-3.7), and let c_h, s_h, z_h be the numerical solution of the semi-discrete LDG scheme (3.11-3.13). If the finite element space is the piecewise polynomials of degree $k \geq 1$, then we have the error estimate

$$\|c - c_h\|_{L^\infty(0,T;L^2)} + \|s - s_h\|_{L^2(0,T;L^2)} \leq Kh^{k+1}, \tag{3.21}$$

where the constant K is dependent upon T and some norms of the solution (c, u) and independent of the mesh parameter h.

Proof: From (3.8)-(3.13), we have the following error equations

$$\int_{I_j}\phi(x)\frac{\partial(c-c_h)}{\partial t}vdx-\int_{I_j}(uc-u_hc_h)v_xdx+(uc-\widehat{u_hc_h})_{j+\frac{1}{2}}v^-_{j+\frac{1}{2}}-(uc-\widehat{u_hc_h})_{j-\frac{1}{2}}v^+_{j-\frac{1}{2}}$$
$$-\int_{I_j}(z-z_h)v_xdx+(z-\widehat{z_h})_{j+\frac{1}{2}}v^-_{j+\frac{1}{2}}-(z-\widehat{z_h})_{j-\frac{1}{2}}v^+_{j-\frac{1}{2}}=\int_{I_j}(\tilde{c}-\tilde{c_h})qvdx, \quad (3.22)$$

$$\int_{I_j}(s-s_h)wdx-\int_{I_j}(c-c_h)w_xdx+(c-\hat{c_h})_{j+\frac{1}{2}}w^-_{j+\frac{1}{2}}-(c-\hat{c_h})_{j-\frac{1}{2}}w^+_{j-\frac{1}{2}}=0, \quad (3.23)$$

$$\int_{I_j}(z-z_h)\psi dx-\int_{I_j}(D(u)s-D(u_h)s_h)\psi dx=0, \quad (3.24)$$

$\forall v,w,\psi\in V_h^k$, where

$$\tilde{c}-\tilde{c_h}=\begin{cases}0, & q>0,\\ c-c_h, & q<0.\end{cases}$$

Denote $e_o=o-o_h=\xi_o-\eta_o(o=c,s,z)$, where $\xi_o=P_h^{(\pm)}o-o_h,\eta_o=P_h^{(\pm)}o-o$.

We recall that we have taken the alternate $\widehat{z_h}=z_h^-,\widehat{c_h}=c_h^+$. Taking the test functions $v=\xi_c,w=\xi_z,\psi=-\xi_s$ and summing over j, we have

$$\begin{aligned}
&\sum_{j=1}^n\int_{I_j}\phi(x)\frac{\partial\xi_c}{\partial t}\xi_cdx+\sum_{j=1}^n\int_{I_j}D(u_h)\xi_s^2dx\\
=\;&\sum_{j=1}^n\int_{I_j}\phi(x)\frac{\partial\eta_c}{\partial t}\xi_cdx+\sum_{j=1}^n\int_{I_j}D(u_h)\eta_s\xi_sdx-\sum_{j=1}^n\int_{I_j}(D(u)-D(u_h))s\xi_sdx\\
&+\sum_{j=1}^n(\int_{I_j}(uc-u_hc_h)(\xi_c)_xdx-(uc-\widehat{u_hc_h})_{j+\frac{1}{2}}\xi_{c\,j+\frac{1}{2}}^-+(uc-\widehat{u_hc_h})_{j-\frac{1}{2}}\xi_{c\,j-\frac{1}{2}}^+)\\
&+[\mathcal{D}(\xi_z,\xi_c;\xi_z^-)+\mathcal{D}(\xi_c,\xi_z;\xi_c^+)]\\
&-[\mathcal{D}(z-P_h^-z,\xi_c;(z-P_h^-z)^-)+\mathcal{D}(c-P_h^+c,\xi_z;(c-P_h^+c)^+)]\\
&+\sum_{j=1}^n\int_{I_j}\eta_s\xi_zdx-\sum_{j=1}^n\int_{I_j}\eta_z\xi_sdx+\sum_{j=1}^n\int_{I_j}(\widetilde{\xi_c}-\widetilde{\eta_c})q\xi_cdx\\
=\;&T_1+T_2+\ldots T_9.
\end{aligned}\quad (3.25)$$

Now, we estimate T_i term by term. Using the projection and the Schwartz inequality, we can get

$$T_1\le K\int_I(\eta_c)_t^2dx+K\int_I\xi_c^2dx\le Kh^{2(k+1)}+K\|\xi_c\|^2, \quad (3.26)$$

$$T_2\le K\int_I\eta_s^2dx+\epsilon\int_I\xi_s^2dx\le Kh^{2(k+1)}+\epsilon\|\xi_s\|^2. \quad (3.27)$$

From (3.15)

$$\begin{aligned} T_3 &\leq K\int_I (D(u)-D(u_h))^2dx + \epsilon\int_I \xi_s^2 dx \leq K\|u-u_h\|^2 + \epsilon\|\xi_s\|^2 \\ &\leq Kh^{2(k+1)} + K\|\xi_c\|^2 + \epsilon\|\xi_s\|^2, \end{aligned} \tag{3.28}$$

where K depends on $\|s\|_\infty$.

$$\begin{aligned} T_4 &= \sum_{j=1}^n (\int_{I_j} (uc-u_hc_h)(\xi_c)_x dx + (uc-\widehat{u_hc_h})_{j+\frac{1}{2}}[\xi_c]_{j+\frac{1}{2}} \\ &= \sum_{j=1}^n \int_{I_j} (u-u_h)c(\xi_c)_x dx + \sum_{j=1}^n \int_{I_j} u_h(\xi_c-\eta_c)(\xi_c)_x dx \\ &\quad + \sum_{j=1}^n (u-u_h)_{j+\frac{1}{2}} c_{j+\frac{1}{2}}[\xi_c]_{j+\frac{1}{2}} + \sum_{j=1}^n u_{hj+\frac{1}{2}}(\widehat{\xi_c}-\widehat{\eta_c})_{j+\frac{1}{2}}[\xi_c]_{j+\frac{1}{2}} \\ &= \sum_{j=1}^n \int_{I_j} u_h\xi_c(\xi_c)_x dx + \sum_{j=1}^n u_{hj+\frac{1}{2}}\widehat{\xi_c}_{j+\frac{1}{2}}[\xi_c]_{j+\frac{1}{2}} \\ &\quad - \sum_{j=1}^n \int_{I_j} u_h\eta_c(\xi_c)_x dx - \sum_{j=1}^n u_{hj+\frac{1}{2}}\widehat{\eta_c}_{j+\frac{1}{2}}[\xi_c]_{j+\frac{1}{2}} \\ &\quad + \sum_{j=1}^n \int_{I_j} (u-u_h)c(\xi_c)_x dx + \sum_{j=1}^n (u-u_h)_{j+\frac{1}{2}} c_{j+\frac{1}{2}}[\xi_c]_{j+\frac{1}{2}} \\ &= T_{41}+T_{42}+\ldots+T_{46}. \end{aligned} \tag{3.29}$$

Recall the upwind flux, that is, if $u_h > 0$, is $\widehat{u_hc_h} = u_hc_h^-$; otherwise, it is $\widehat{u_hc_h} = u_hc_h^+$. Integrating by parts, we have

$$\begin{aligned} T_{41}+T_{42} &= -\frac{1}{2}\sum_{j=1}^n \int_{I_j} (u_h)_x\xi_c^2 dx - \frac{1}{2}\sum_{j=1}^n u_{hj+\frac{1}{2}}[\xi_c^2]_{j+\frac{1}{2}} + \sum_{j=1}^n u_{hj+\frac{1}{2}}\widehat{\xi_c}_{j+\frac{1}{2}}[\xi_c]_{j+\frac{1}{2}} \\ &= -\frac{1}{2}\sum_{j=1}^n \int_{I_j} (u_h)_x\xi_c^2 dx - \frac{1}{2}\sum_{j=1}^n |u_{hj+\frac{1}{2}}|[\xi_c]_{j+\frac{1}{2}}^2 \\ &\leq K\|\xi_c\|^2 - \frac{1}{2}\sum_{j=1}^n |u_{hj+\frac{1}{2}}|[\xi_c]_{j+\frac{1}{2}}^2, \end{aligned} \tag{3.30}$$

where K depends on $\|(u_h)_x\|_\infty$. Lemma 3.1 implies that $\|(u_h)_x\|_\infty \leq K$. Noticing that $|u_h - u_{hj+\frac{1}{2}}| = O(h)$ on each element I_j, we have

$$\begin{aligned} T_{43} &= -\sum_{j=1}^n \int_{I_j} (u_h - u_{hj+\frac{1}{2}})\eta_c(\xi_c)_x dx - \sum_{j=1}^n \int_{I_j} u_{hj+\frac{1}{2}}\eta_c(\xi_c)_x dx \\ &= -\sum_{j=1}^n \int_{I_j} (u_h - u_{hj+\frac{1}{2}})\eta_c(\xi_c)_x dx \\ &\leq K\|\xi_c\|^2 + Kh^{2(k+1)}, \end{aligned} \tag{3.31}$$

where the first equality is trivial, the second one follows from the property of the projection and the last inequality is based on the inverse property, together with the property of the projection and Schwartz inequality.

$$\begin{aligned} T_{44} &= \sum_{j=1}^{n}(u-u_h)_{j+\frac{1}{2}}\widehat{\eta_c}_{j+\frac{1}{2}}[\xi_c]_{j+\frac{1}{2}} - \sum_{j=1}^{n} u_{j+\frac{1}{2}}\widehat{\eta_c}_{j+\frac{1}{2}}[\xi_c]_{j+\frac{1}{2}} \\ &= T_{441} + T_{442}. \end{aligned} \tag{3.32}$$

Noticing that $\|u-u_h\|_{0,\infty} = O(h)$, then by the inverse property, together with the property of the projection and Schwartz inequality, we have

$$T_{441} \leq K\|\xi_c\|^2 + Kh^{2(k+1)}. \tag{3.33}$$

I: In case $u > 0$ on $I_j \cup I_{j+1}$, $\widehat{\eta_c} = \eta_c^-$, then $T_{442} = 0$.
II: In case $u < 0$ on $I_j \cup I_{j+1}$, $\widehat{\eta_c} = \eta_c^+$, then $T_{442} = 0$.
III: In case the sign of u is changed, then $|u_{j+\frac{1}{2}}| = O(h)$, then

$$T_{442} \leq K\|\xi_c\|^2 + Kh^{2(k+1)}. \tag{3.34}$$

Then we obtain

$$T_{44} \leq K\|\xi_c\|^2 + Kh^{2(k+1)}. \tag{3.35}$$

$$\begin{aligned} & T_{45} + T_{46} \\ = & -\sum_{j=1}^{n}\int_{I_j}((u-u_h)c)_x\xi_c dx - \sum_{j=1}^{n}(u-u_h)_{j+\frac{1}{2}}c_{j+\frac{1}{2}}[\xi_c]_{j+\frac{1}{2}} + \sum_{j=1}^{n}(u-u_h)_{j+\frac{1}{2}}c_{j+\frac{1}{2}}[\xi_c]_{j+\frac{1}{2}} \\ = & -\sum_{j=1}^{n}\int_{I_j}(u-u_h)_x c\xi_c dx - \sum_{j=1}^{n}\int_{I_j}(u-u_h)c_x\xi_c dx \\ \leq & K\|\xi_c\|^2 + K\|(u-u_h)_x\|^2 + K\|u-u_h\|^2 \\ \leq & K\|\xi_c\|^2 + Kh^{2k+2}, \end{aligned} \tag{3.36}$$

where K depends on $\|c\|_\infty$ and $\|c_x\|_\infty$. Then substituting (3.30)-(3.36) into (3.29), we have

$$T_4 \leq K\|\xi_c\|^2 + Kh^{2(k+1)} - \frac{1}{2}\sum_{j=1}^{n}|u_{h_{j+\frac{1}{2}}}|[\xi_c]^2_{j+\frac{1}{2}}. \tag{3.37}$$

Using the property of the operator $\mathcal{D}$ in Lemma 3.2, we can get

$$T_5 = 0. \tag{3.38}$$

Obviously, it follows from the Lemma 3.3, that

$$T_6 = 0.$$

Using the projection and the Schwartz inequality, we easily obtain

$$T_7 \le K\int_I \eta_s^2 dx + \epsilon\int_I \xi_z^2 dx \le Kh^{2(k+1)} + \epsilon\|\xi_z\|^2, \tag{3.39}$$

$$T_8 \le K\int_I \eta_z^2 dx + \epsilon\int_I \xi_s^2 dx \le Kh^{2(k+1)} + \epsilon\|\xi_s\|^2, \tag{3.40}$$

$$T_9 \le K\int_I \eta_c^2 dx + K\int_I \xi_c^2 dx \le Kh^{2(k+1)} + K\|\xi_c\|^2. \tag{3.41}$$

Substituting the estimation (3.26)-(3.41) into (3.25), we obtain

$$\begin{aligned} &\frac{d}{dt}\|\phi^{\frac{1}{2}}\xi_c\| + \|D^{\frac{1}{2}}(u_h)\xi_s\|^2 + \frac{1}{2}\sum_{j=1}^{n}|u_{h_{j+\frac{1}{2}}}|[\xi_c]^2_{j+\frac{1}{2}} \\ \le\ & K\|\xi_c\|^2 + \epsilon\|\xi_s\|^2 + \epsilon\|\xi_z\|^2 + Kh^{2(k+1)}. \end{aligned} \tag{3.42}$$

Setting $\psi = \xi_z$ in (3.24) and summing over j, we have

$$\begin{aligned} \sum_{j=1}^{n}\int_{I_j}\xi_z^2 dx &= \sum_{j=1}^{n}\int_{I_j}\eta_z\xi_z dx + \sum_{j=1}^{n}\int_{I_j}(D(u)s - D(u_h)s_h)\xi_z dx \\ &= P_1 + P_2. \end{aligned} \tag{3.43}$$

Using the projection and the Schwartz inequality, we can get

$$P_1 \le K\int_I \eta_z^2 dx + \epsilon\int_I \xi_z^2 dx \le Kh^{2(k+1)} + \epsilon\|\xi_z\|^2, \tag{3.44}$$

$$\begin{aligned} P_2 &= \sum_{j=1}^{n}\int_{I_j}(D(u) - D(u_h))s\xi_z dx + \sum_{j=1}^{n}\int_{I_j}D(u_h)(s - s_h)\xi_z dx \\ &= P_{21} + P_{22}. \end{aligned} \tag{3.45}$$

From (3.15) in lemma 3.1

$$\begin{aligned} P_{21} &\le K\int_I (D(u) - D(u_h))^2 dx + \epsilon\int_I \xi_z^2 dx \le K\|u - u_h\|^2 + \epsilon\|\xi_z\|^2 \\ &\le Kh^{2(k+1)} + K\|\xi_c\|^2 + \epsilon\|\xi_z\|^2, \end{aligned} \tag{3.46}$$

where K is dependent on $\|s\|_\infty$.

$$P_{22} \le K\int_I \eta_s^2 dx + K\int_I \xi_s^2 dx + \epsilon\int_I \xi_z^2 dx \le Kh^{2(k+1)} + K\|\xi_s\|^2 + \epsilon\|\xi_z\|^2. \tag{3.47}$$

Substituting the estimation (3.44)-(3.47) into (3.43), we obtain

$$\|\xi_z\|^2 \quad \leq \quad Kh^{2(k+1)} + K\|\xi_c\|^2 + K\|\xi_s\|^2. \tag{3.48}$$

Combing (3.42) and (3.48), we obtain

$$\begin{aligned} & \frac{d}{dt}\|\phi^{\frac{1}{2}}\xi_c\| + \|D^{\frac{1}{2}}(u_h)\xi_s\|^2 + \frac{1}{2}\sum_{j=1}^{n} |u_{h\,j+\frac{1}{2}}|[\xi_c]^2_{j+\frac{1}{2}} \\ \leq \quad & K\|\xi_c\|^2 + \epsilon\|\xi_s\|^2 + Kh^{2(k+1)}. \end{aligned} \tag{3.49}$$

Integrating with respect to time between 0 and t and using the initial approximation and the Gronwall lemma, we obtain

$$\|\xi_c\|_{L^\infty(0,T;L^2)} + \|\xi_s\|_{L^2(0,T;L^2)} \leq Kh^{k+1}. \tag{3.50}$$

To complete the proof, let us verify the a-priori assumption (3.14). For $k \geq 1$, we can consider h small enough so that $Kh^{k+1} < \frac{1}{2}h^{\frac{3}{2}}$, where K is the constant determined by the final time T. Then if $t^* = \sup\{t : \|u - u_h\| \leq h^{\frac{3}{2}}\}$, we should have $\|(u-u_h)(t^*)\| = h^{\frac{3}{2}}$ by continuity if t^* is finite. However, our proof implies that $\|u - u_h\| \leq Kh^{k+1}$ for $t \leq t^*$, in particular $\|(u - u_h)(t^*)\| \leq Kh^{k+1} < \frac{1}{2}h^{\frac{3}{2}}$, which is a contradiction. Therefore, there always holds $t^* \geq T$, and thus the a priori assumption (3.14) is justified.

3.3. Numerical example

In this section we provide numerical examples to illustrate the accuracy and capability of the method. Time discretization is by the third order explicit Runge-Kutta method in [26]. With a sufficiently small time step so that error in time is negligible compared spatial errors. In the scheme ,we choose $\widehat{u_h c_h} = \max(u_h, 0)c_h^- + \min(u_h, 0)c_h^+$, $\widehat{z_h} = z_h^-, \widehat{c_h} = c_h^+$. We implemented a slope-limiting procedure at each step of the calculation to prevent spurious oscillations.

$$\begin{aligned} u^-_{j+\frac{1}{2}} &= \bar{v}_j + \tilde{m}(v^-_{j+\frac{1}{2}} - \bar{v}_j, \bar{v}_j - \bar{v}_{j-1}, \bar{v}_{j+1} - \bar{v}_j), \\ u^+_{j-\frac{1}{2}} &= \bar{v}_j - \tilde{m}(\bar{v}_j - v^+_{j-\frac{1}{2}}, \bar{v}_j - \bar{v}_{j-1}, \bar{v}_{j+1} - \bar{v}_j), \end{aligned}$$

$$\tilde{m}(a_1, \cdots, a_m) = \begin{cases} a_1, & \text{if} \quad |a_1| \leq M(\Delta x)^2, \\ m(a_1, \cdots, a_m), & \text{otherwise}, \end{cases}$$

$$m(a_1, \cdots, a_\nu) = \begin{cases} \min\limits_{1\leq n\leq \nu} |a_n|, & \text{if} \quad s = \text{sign}(a_1) \cdots = \text{sign}(a_\nu), \\ 0, & \text{otherwise}, \end{cases}$$

where constant M is an upper bound of the absolute value of the second-order derivative of the solution at the local extrema.

Example 1. We first consider a smooth test problem

$$\begin{cases} \partial_t c + u\partial_x c - D\partial_{xx} c = 0, & x \in \Omega, \quad 0 < t \leq T, \\ c(x,0) = \sin x, & x \in \Omega, \end{cases} \tag{3.51}$$

where $\Omega = (0, 2\pi]$, $c(0,t) = c(2\pi,t)$, u and D are constants, the exact solution is $c = e^{-Dt}\sin(x-t)$. The L^2 error and the numerical orders of accuracy at time $t = 1.0$ with uniform meshes are contained in Tables 1-4. We can see that the method with P^k elements gives $(k+1)$th order of accuracy in L^2 norm.

Table 1: The numerical results for c with $u = 1.0, D = 0.0$.

N	P^1		P^2		P^3	
	L^2 error	order	L^2 error	order	L^2 error	order
10	1.6446E-02	–	8.5981E-04	–	3.5317E-05	–
20	4.2128E-03	1.96	1.0697E-04	3.01	2.0674E-06	4.09
40	1.0597e-03	1.99	1.3372e-05	3.00	1.3038e-07	3.99
80	2.6532e-04	2.00	1.6716e-06	3.00	8.0710e-09	4.01
160	6.6354e-05	2.00	2.0895e-07	3.00	5.0444e-10	4.00

Table 2: The numerical results for c with $u = 0.0, D = 1.0$.

N	$P1$		$P2$		$P3$	
	L^2 error	order	L^2 error	order	L^2 error	order
10	6.2848E-03	–	3.1505E-04	–	1.2137E-05	–
20	1.5646e-03	2.01	3.9361e-05	3.00	7.5972e-07	4.00
40	3.9074e-04	2.00	4.9197e-06	3.00	4.7500e-08	4.00
80	9.7662e-05	2.00	6.1495e-07	3.00	2.9690e-09	4.00
160	2.4414e-05	2.00	7.6868e-08	3.00	1.8572e-10	4.00

Table 3: The numerical results for c with $u = 1.0, D = 0.01$.

N	$P1$		$P2$		$P3$	
	L^2 error	order	L^2 error	order	L^2 error	order
10	1.6392E-02	–	8.4284E-04	–	3.3575E-05	–
20	4.1845e-03	1.97	1.0559e-04	3.00	2.0464e-06	4.04
40	1.0505e-03	1.99	1.6545e-05	3.00	1.2787e-07	4.00
80	2.6280e-04	2.00	1.6545e-06	3.00	7.9905e-09	4.00
160	6.5704e-05	2.00	2.0686e-07	3.00	4.9942e-10	4.00

Table 4: The numerical results for c with $u = 1.0, D = 1.0$.

N	$P1$		$P2$		$P3$	
	L^2 error	order	L^2 error	order	L^2 error	order
10	6.3335E-03	–	3.1488E-04	–	1.2136E-05	–
20	1.5681e-03	2.01	3.9359e-05	3.00	7.5971e-07	4.00
40	3.9098e-04	2.00	4.9197e-06	3.00	4.7500e-08	4.00
80	9.7677e-05	2.00	6.1495e-07	3.00	2.9690e-09	4.00
160	2.4415e-05	2.00	7.6868e-08	3.00	1.8574e-10	4.00

Example 2. Here we consider the problem

$$\begin{cases} \partial_t c + \partial_x(uc) - D\partial_{xx}c = cq + f(x,t), & x \in \Omega, \quad 0 < t \leq T, \\ c(x,0) = \sin x, & x \in \Omega, \\ u_x = q, & x \in \Omega, \end{cases} \tag{3.52}$$

where $\Omega = (0, 2\pi]$, $c(0,t) = c(2\pi,t)$, $f(x,t) = e^{-t}(\cos(x-t)(\sin x - 1) + (D-1)\sin(x-t))$, $u = \sin x, q = \cos x$, the exact solution is $c = e^{-t}\sin(x-t)$. The L^2 error and the numerical orders of accuracy at time $t = 1.0$ with uniform meshes are contained in Tables 5-7. We can see that the method with P^k elements gives $(k+1)$th order of accuracy in L^2 norm.

Table 5: The numerical results for c with $D = 1.0$.

N	P^1		P^2		P^3	
	L^2 error	order	L^2 error	order	L^2 error	order
10	6.1175E-03	–	3.0868E-04	–	1.2044E-05	–
20	1.5399e-03	1.99	3.8896e-05	2.99	7.5568e-07	3.99
40	3.8744e-04	1.99	4.8886e-06	2.99	4.7355e-08	4.00
80	9.7236e-05	1.99	6.1296e-07	3.00	2.9642e-09	4.00
160	2.4360e-05	2.00	7.6742e-08	3.00	1.8553e-10	4.00

Table 6: The numerical results for c with $D = 0.01$.

N	P^1		P^2		P^3	
	L^2 error	order	L^2 error	order	L^2 error	order
10	6.2387E-03	–	5.5587E-04	–	3.9913E-05	–
20	1.4642e-03	2.09	4.9249e-05	3.50	1.4956e-06	4.74
40	3.4185e-04	2.10	4.8653e-06	3.34	7.8774e-08	4.25
80	8.4313e-05	2.02	5.7729e-07	3.08	4.1333e-09	4.25
160	2.1658e-05	2.00	7.1068e-08	3.02	2.1460e-10	4.27

Table 7: The numerical results for c with $D = 0.0$.

N	P^1		P^2		P^3	
	L^2 error	order	L^2 error	order	L^2 error	order
10	6.2387E-03	–	7.0191E-04	–	6.5558E-05	–
20	1.6988e-03	2.15	7.5818e-05	3.21	2.9595e-06	4.47
40	4.0671e-04	2.06	7.8794e-06	3.27	1.5349e-07	4.27
80	9.9719e-05	2.03	8.3247e-07	3.24	8.4131e-09	4.19
160	2.1658e-05	2.00	9.1819e-08	3.18	4.7925e-10	4.13

Example 3. Here we consider the problem

$$\begin{cases} \partial_x u = q, & x \in \Omega, \quad t > 0, \\ \partial_t c + \partial_x(uc) - \partial_x(D(u)\partial_x c) = cq + f(x,t), & x \in \Omega, \quad t > 0, \\ c(x,0) = \sin x, \end{cases} \tag{3.53}$$

where $\Omega = (0, 2\pi]$, $c(0,t) = c(2\pi,t)$, $q = \cos x$, $D(u) = u^2 + 1$, $f(x,t) = e^{-t}(\cos(x - t)(\sin x - 1 - 2\sin x\cos x) + (D(u) - 1)\sin(x - t)$. The exact solution is $c = e^{-t}\sin(x - t)$. The L^2 error and the numerical orders of accuracy at time $t = 1.0$ with uniform meshes are contained in Table 8. We can see that the method with P^k elements gives $(k + 1)$th order of accuracy in L^2 norm.

Table 8: The numerical results for c .

N	P^1		P^2		P^3	
	L^2 error	order	L^2 error	order	L^2 error	order
10	6.3136e-03	–	3.3125e-04	–	1.5003e-05	–
20	1.5597e-03	2.02	3.9730e-05	3.06	8.0524e-07	4.22
40	3.8926e-04	2.00	4.9178e-06	3.01	4.8075e-08	4.07
80	9.7412e-05	2.00	6.1401e-07	3.00	2.9726e-09	4.02
160	2.4378e-05	2.00	7.6784e-08	3.00	1.8553e-10	4.00

Example 4. Here we consider the problem

$$\begin{cases} \partial_t c + u\partial_x c - D\partial_{xx} c = 0, & 0 < x \leq \pi, \quad t > 0, \\ c(x,0) = 0, \\ (uc - Dc_x)(0,t) = u, c(\pi,t) = 0. \end{cases} \tag{3.54}$$

Fig. 1 shows the approximate solution, on meshes of 40, 80 and 160 equally spaced element, with $u = 1.0$ and $D = 1.0$, at $t = 1.1$, $t = 3.1$ and $t = 5.1$. Then we consider a convection dominated case with $u = 1.0$ and $D = 0.001$. Fig. 2 shows the approximate solution, on meshes of 40, 80 equally spaced element at five points in time.

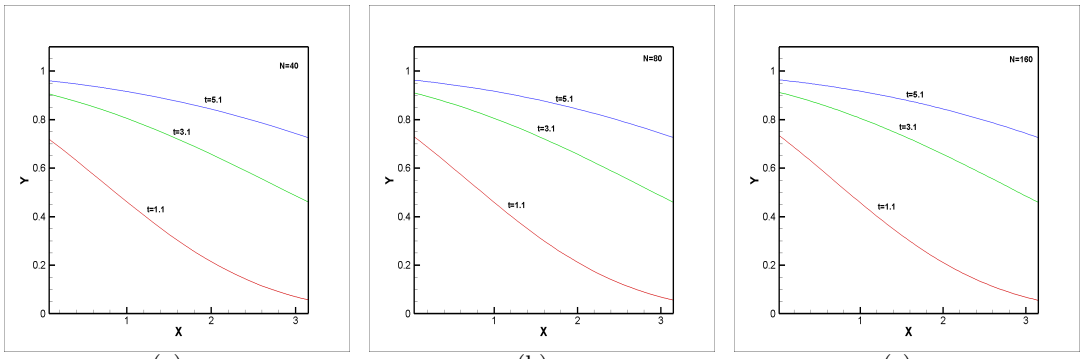

(a) (b) (c)

Figure 1: Approximate solution to convection diffusion case.

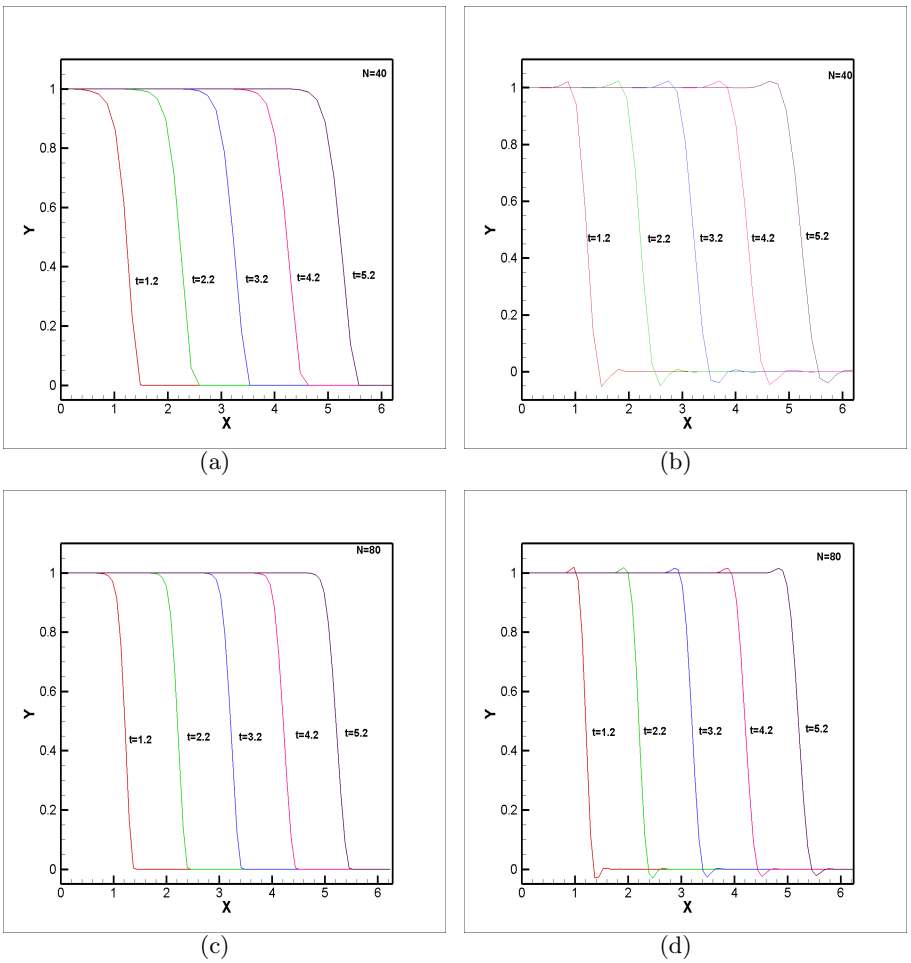

(a) (b) (c) (d)

Figure 2: Approximate solutions to convection dominated case: (a) and (c) limiter, (b) and (d) no limiter

Example 5. Here we consider the same problem as above, with the initial condition

$$c(x,0) = \begin{cases} 1, 0 < x < 0.5, \\ 0, \text{otherwise} \end{cases}$$

and boundary conditions $(uc - Dc_x)(0,t) = 0, c(\pi,t) = 0$. We again take $u = 1.0$ and $D = 0.001$. Fig. 3 shows the approximate solution, on meshes of 80, 160 and 320 equally spaced element at five points in time.

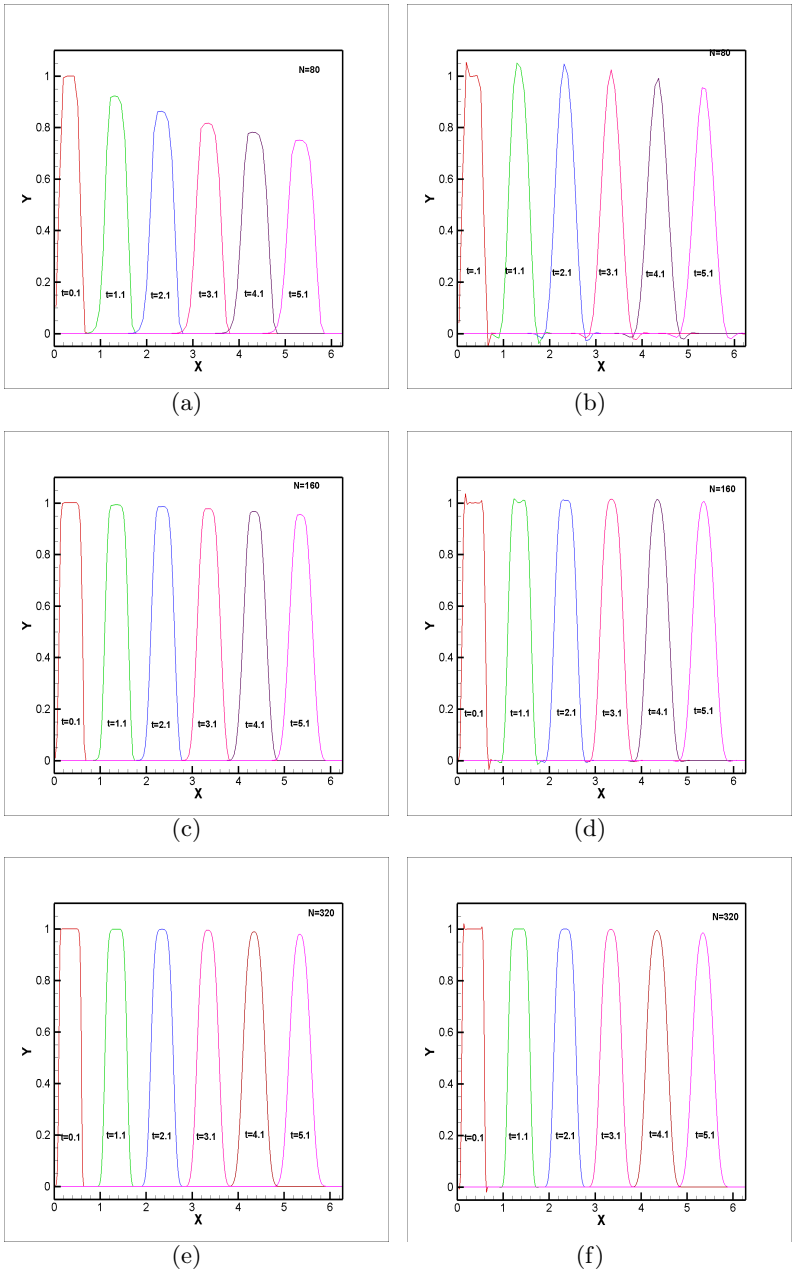

Figure 3: Approximate solutions to convection dominated case:(a), (c) and (e) limiter; (b), (d) and (f) no limiter

4. Compressible miscible displacement problem

In this section, we give the analysis for the one-dimensional compressible miscible displacement problem. Detailed discussion on physical theories of miscible displacement in porous media can be found in [27]

$$d(c)\frac{\partial p}{\partial t} + u_x = d(c)\frac{\partial p}{\partial t} - (\frac{k(x)}{\mu(c)}p_x)_x = q, \quad x \in I, \quad 0 < t \leq T, \tag{4.1}$$

$$\phi(x)\frac{\partial c}{\partial t} + b(c)\frac{\partial p}{\partial t} + u \cdot c_x - (D(u)c_x)_x = (\tilde{c} - c)q, \quad x \in I, \quad 0 < t \leq T. \tag{4.2}$$

In the above model, we confine ourselves to a two component displacement problem just for clarity of presentation. However, the numerical methods that we shall introduce and analyze below can be applied to the n component model. The coefficients can be stated as follows:

$$\begin{aligned} &c = c_1 = 1 - c_2, \\ &b(c) = b(x,c) = \phi(x)c_1\{z_1 - \sum_{j=1}^{2} z_j c_j\}, \\ &d(c) = d(x,c) = \phi(x)\sum_{j=1}^{2} z_j c_j, \end{aligned}$$

where c_i denote the concentration of the i th component of the fluid mixture, and z_i is the "constant compressibility" factor. The definition $\phi(x), \mu(c), k(x), D(u), q$ and $\tilde{c}$ are just like the definition of incompressible miscible displacement model.

We also assume that the problem is periodic in space. In addition, the initial conditions are

$$\begin{aligned} &c(x,0) = c_0(x), \quad x \in I, \\ &p(x,0) = p_0(x), \quad x \in I. \end{aligned}$$

4.1. Weak form and the LDG scheme

First, the mixed finite element method is used to solve the flow equation: find $(u_h, p_h) \in W_h^{k+1} \times Z_h^k$ such that

$$\begin{aligned} &(\mu(c_h)k(x)^{-1}u_h, \theta) - (\theta_x, p_h) = 0, \quad \forall \theta \in W_h^{k+1}, \\ &(d(c_h)\frac{\partial p_h}{\partial t}, \zeta) + ((u_h)_x, \zeta) = (q, \zeta), \quad \forall \zeta \in Z_h^k, \end{aligned} \tag{4.3}$$

where $W_h^{k+1} = \{\theta \in C^0(I) : \theta|_{I_j} \in P^{k+1}(I_j)\}, Z_h^k = \{\zeta \in L^2(I) : \zeta|_{I_j} \in P^k(I_j)\} = V_h^k$.

Since $cq = cd(c)\frac{\partial p}{\partial t} + c\frac{\partial u}{\partial x}$, then the equation (4.2) can be changed to

$$\phi(x)\frac{\partial c}{\partial t} + B(c)\frac{\partial p}{\partial t} + (uc)_x - (D(u)c_x)_x = \tilde{c}q, \tag{4.4}$$

where $B(c) = b(c) + cd(c)$.

To construct the LDG method, firstly we rewrite the equation (4.4) as a system containing only first order derivatives:

$$\phi(x)\frac{\partial c}{\partial t} + B(c)\frac{\partial p}{\partial t} + (uc)_x + z_x = \tilde{c}q, \tag{4.5}$$

$$s = -c_x, \tag{4.6}$$

$$z = D(u)s. \tag{4.7}$$

We multiply equations (4.5)-(4.7) by test functions v, w, ψ respectively, and formally integrate by parts for all terms involving a spatial derivative to get

$$\begin{aligned}\int_{I_j} \phi(x)\frac{\partial c}{\partial t}v dx + \int_{I_j} B(c)\frac{\partial p}{\partial t}v dx - \int_{I_j} ucv_x dx + (uc)_{j+\frac{1}{2}}v^-_{j+\frac{1}{2}} - (uc)_{j-\frac{1}{2}}v^+_{j-\frac{1}{2}} \\ - \int_{I_j} zv_x dx + z_{j+\frac{1}{2}}v^-_{j+\frac{1}{2}} - z_{j-\frac{1}{2}}v^+_{j-\frac{1}{2}} = \int_{I_j} \tilde{c}qv dx,\end{aligned} \tag{4.8}$$

$$\int_{I_j} sw dx - \int_{I_j} cw_x dx + c_{j+\frac{1}{2}}w^-_{j+\frac{1}{2}} - c_{j-\frac{1}{2}}w^+_{j-\frac{1}{2}} = 0, \tag{4.9}$$

$$\int_{I_j} z\psi dx - \int_{I_j} D(u)s\psi dx = 0. \tag{4.10}$$

Replacing the exact solutions u, c, s and z in the above equations by their numerical approximations u_h, c_h, s_h and z_h, noticing that the numerical solutions c_h, s_h and z_h are not continuous on the cell boundaries, then replacing terms on the cell boundaries by suitable numerical fluxes, we obtain the LDG scheme:

$$\begin{aligned}\int_{I_j} \phi(x)\frac{\partial c_h}{\partial t}v dx + \int_{I_j} B(c_h)\frac{\partial p_h}{\partial t}v dx \\ - \int_{I_j} u_h c_h v_x dx + (\widehat{u_h c_h})_{j+\frac{1}{2}}v^-_{j+\frac{1}{2}} - (\widehat{u_h c_h})_{j-\frac{1}{2}}v^+_{j-\frac{1}{2}} \\ - \int_{I_j} z_h v_x dx + \widehat{z_h}_{j+\frac{1}{2}}v^-_{j+\frac{1}{2}} - \widehat{z_h}_{j-\frac{1}{2}}v^+_{j-\frac{1}{2}} = \int_{I_j} \tilde{c_h}qv dx,\end{aligned} \tag{4.11}$$

$$\int_{I_j} s_h w dx - \int_{I_j} c_h w_x dx + \hat{c_h}_{j+\frac{1}{2}}w^-_{j+\frac{1}{2}} - \hat{c_h}_{j-\frac{1}{2}}w^+_{j-\frac{1}{2}} = 0, \tag{4.12}$$

$$\int_{I_j} z_h \psi dx - \int_{I_j} D(u_h)s_h\psi dx = 0, \tag{4.13}$$

The important thing is that $\widehat{u_h c_h}$ should be chosen based on upwinding, $\widehat{u_h c_h} = \max(u_h, 0)c_h^- + \min(u_h, 0)c_h^+$ and $\widehat{z_h}$ and $\widehat{c_h}$ should be chosen alternatively from the left and the right.

4.2. Numerical example

In this section we provide numerical examples to illustrate the accuracy and capability of the method for compressible miscible displacement problem. Time discretization is by the third order explicit Runge-Kutta method in [26], with a sufficiently small time step so that error in time is negligible compared to spatial errors. In the LDG method, we implemented a slope-limiting procedure at each step of the calculation to prevent spurious oscillations as before.

Example 6. Here we consider the problem:

$$\begin{cases} \partial_t p + \partial_x u = q, & 0 < x < 2\pi, \quad t > 0, \\ \partial_t c + \partial_t p + u\partial_x c - D\partial_{xx} c = (\tilde{c} - c)q, & 0 < x < 2\pi, \quad t > 0, \\ u = -\partial_x p, \\ c(x,0) = \sin x, \\ p(x,0) = \cos x, \end{cases} \tag{4.14}$$

where $q = \sin(x-t) + \cos(x-t)$, $\tilde{c}q = \sin(x-t) + (D - 1 + \sin(x-t))e^{-t}\sin(x-t) - e^{-t}\cos(x-t) + 2\sin^2(x-t)e^{-t}$, the exact solution is $c = e^{-t}\sin(x-t)$, $p = \cos(x-t)$. We choose $\widehat{z_h} = z_h^-, \widehat{c_h} = c_h^+$. The L^2 error and the numerical orders of accuracy at time $t = 1.0$ with uniform meshes are contained in Table 9. We can see that the method with P^1 elements gives 2nd order of accuracy in L^2 norm.

Table 9: The numerical results for c with $D = 1.0$.

N	$P^1(D = 1.0)$		$P^1(D = 0.1)$	
	L^2 error	order	L^2 error	order
10	6.0626E-03	–	5.7691E-03	–
20	1.5288e-03	1.99	1.3798e-03	2.06
40	3.8579e-04	1.99	3.5533e-04	1.96
80	9.7013e-05	1.99	9.2193e-05	1.95

Example 7. Here we consider the problem :

$$\begin{cases} \partial_t p + \partial_x u = q, & 0 < x < 2\pi, \quad t > 0, \\ \partial_t c + \partial_t p + u\partial_x c - \partial_x(D(u)\partial_x c) = (\tilde{c} - c)q, & 0 < x < 2\pi, \quad t > 0, \\ u = -\partial_x p, \\ c(x,0) = \sin x, \\ p(x,0) = \cos x, \end{cases} \tag{4.15}$$

where $q = \sin(x-t) + \cos(x-t)$, $\tilde{c}q = \sin(x-t) + (D(u) - 1 + \sin(x-t))e^{-t}\sin(x-t) - e^{-t}\cos(x-t) + 2\sin(x-t)\cos(x-t)e^{-t} - 2\sin(x-t)\cos(x-t)e^{-t}\cos(x-t)$, $D(u) = u^2 + 1$. The true solution is $c = e^{-t}\sin(x-t)$, $p = \cos(x-t)$. We choose $\widehat{z_h} = z_h^-, \widehat{c_h} = c_h^+$. We can see that the method with P^1 elements gives 2nd order of accuracy in L^2 norm.

Table 10: The numerical results for c with $D(u) = u^2 + 1$.

N	P^1	
	L^2 error	order
10	6.3222E-03	–
20	1.5573e-03	2.02
40	3.8883e-04	2.00
80	9.7352e-05	2.00
160	2.4371e-05	2.00

Example 8. Here we consider the problem:

$$\begin{cases} \partial_t p = q, & 0 < x < \pi, \quad t > 0, \\ \partial_t c - \dfrac{1}{2}\partial_t p + u\partial_x c - D\partial_{xx} c = -\dfrac{q}{2}, & 0 < x < \pi, \quad t > 0, \\ c(x,0) = 0, \\ (uc - D\partial_x c)(0,t) = u, \\ p(x,0) = -\cos x, \end{cases} \tag{4.16}$$

where $q = e^{-t}\sin x$. We take $\widehat{z_h} = z_h^+, \widehat{c_h} = c_h^-$. Fig. 4 shows the approximate solution, on meshes of 40, 80, 160 equally spaced elements, with $u = 1.0$ and $D = 1.0$, at three points in time. Fig. 5 shows the approximate solution, on meshes of 40, 80 equally spaced element, with $u = 1.0$ and $D = 0.001$, at five points in time.

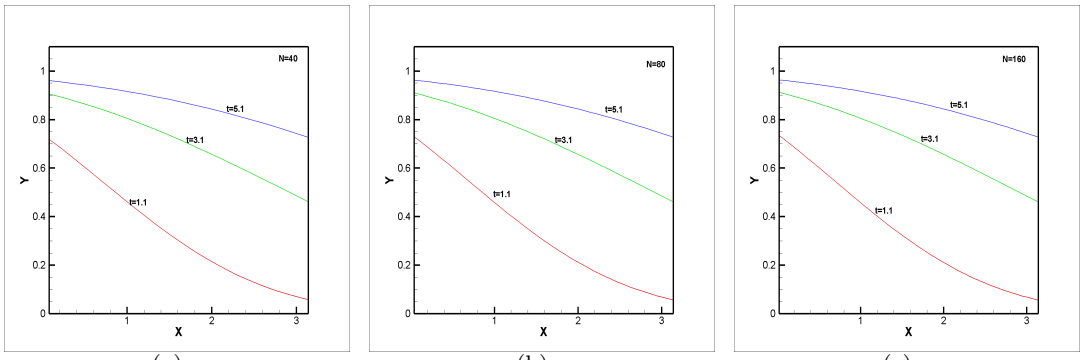

(a) (b) (c)

Figure 4: Approximate solution to convection diffusion case

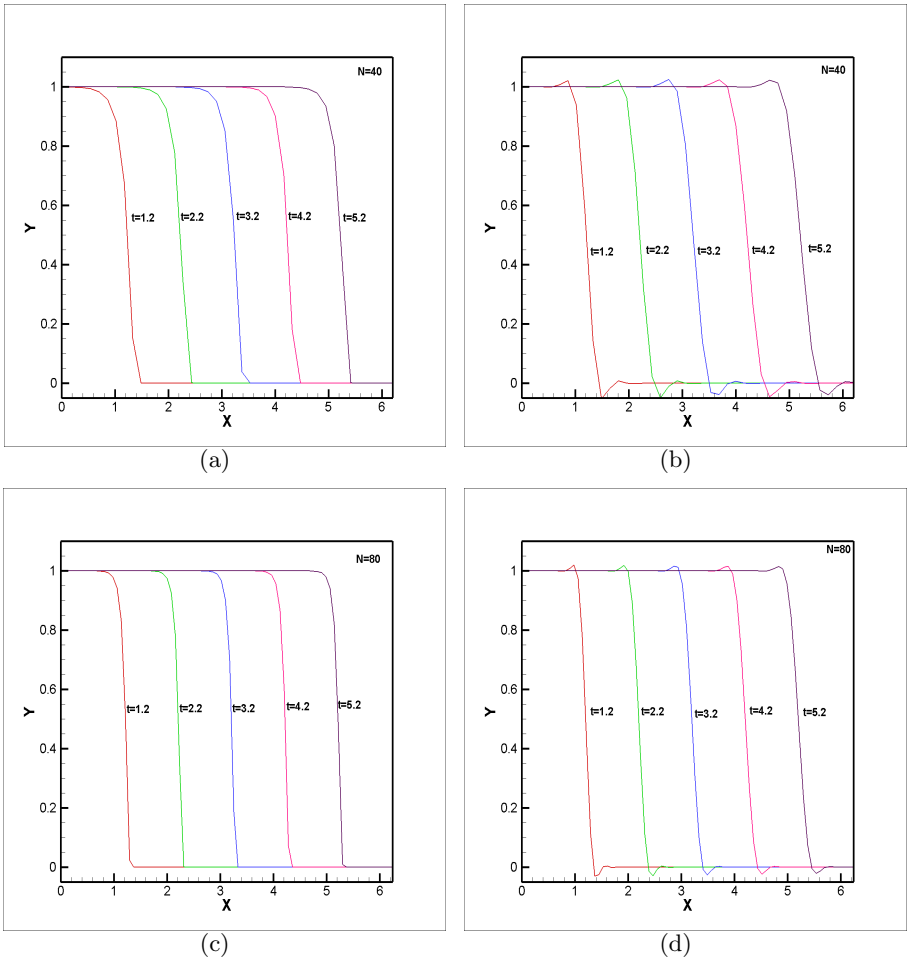

Figure 5: Approximate solutions to convection dominated case: (a) and (c)limiter, (b) and (d)no limiter

5. Concluding remarks

In this paper, a combined method consisting of the mixed finite element method for flow and the LDG method for transport is introduced for the one-dimensional coupled system of incompressible and compressible miscible displacement problem. The optimal order of error estimates hold not only for the solution itself but also for the auxiliary variables for incompressible miscible displacement problem. Special projections and a-priori assumption help to eliminate the jump terms at the cell boundaries. A simulation is performed to two models. It is a challenge to apply this method to the models where $D(u)$ is only positive semi-definite, which will be carried out in future work. Future work will include the study for multi-dimensional miscible displacement problem in porous media, in which the treatment for the auxiliary variables for mixed derivatives should be carried

out carefully in order not to lose half an order or even one order in accuracy.

Acknowledgments

This work was supported by the National Natural Science Foundation of China (No. 11101431) and the Fundamental Research Funds for the Central Universities. The author would like to express sincere thanks to the referees for valuable comments and suggestions.

A Appendix. Proof of lemma 3.1

We proof lemma 3.1 using the technique in [28]. We briefly sketch it for the sake of completeness. From (3.1) and (3.4), we obtain

$$(\mu(c)k^{-1}u - \mu(c_h)k^{-1}u_h, \theta) - (\theta_x, p - p_h) = 0, \forall \theta \in W_h^{k+1}, \tag{A.1}$$

$$((u - u_h)_x, \zeta) = 0, \forall \zeta \in Z_h^k. \tag{A.2}$$

Let $\Re_h : H^1(I_j) \longrightarrow W_h^{k+1}$ be the projection operator defined by

$$\int_{I_j} (z - \Re_h z) q dx = 0, \forall q \in P^{k-1}(I_j), \tag{A.3}$$

$$\Re_h z(x_{j-\frac{1}{2}}) = z(x_{j-\frac{1}{2}}), \Re_h z(x_{j+\frac{1}{2}}) = z(x_{j+\frac{1}{2}}). \tag{A.4}$$

For $k = 0$ the definition of $\Re_h$ reduces to that of the standard conforming interpolant. It is easy to verify that $\Re_h$ corresponds to the one dimensional Raviart-Thomas projection. In particular it satisfies the approximation property

$$\|z - \Re_h z\| \leq K h^{k+1} \|z\|_{k+1}, \forall z \in H^{k+1}(\Omega). \tag{A.5}$$

From the definition of $\Re_h$, it is straightforward to verify that

$$\int_{\Omega} (z - \Re_h z)_x \zeta dx = 0, \forall z \in H^1(\Omega), \forall \zeta \in Z_h^k, \tag{A.6}$$

which express the commuting property of the projection $\frac{d}{dx}(\Re_h z) = P_h(z_x)$, for all $z \in W_h^{k+1}$, P_h being the standard L^2 projection. Combing (A.6) with $z = u$ and equation (A.2), we obtain

$$\int_{\Omega} (\Re_h u - u_h)_x \zeta dx = 0, \forall \zeta \in Z_h^k, \tag{A.7}$$

and so, by setting in $\zeta = (\Re_h u - u_h)_x \in \frac{d}{dx} W_h^{k+1} = Z_h^k$, we have

$$\|(u - u_h)_x\| \leq K h^{k+1} \|u_x\|_{k+1}. \tag{A.8}$$

We next give the L^2 error estimate. Let $\xi_u = \Re_h u - u_h, \eta_u = u - \Re_h u, \xi_p = P_h p - p_h, \eta_p = p - P_h p$. By setting $\zeta = \xi_p$ in (A.7), we have $((\xi_u)_x, \xi_p) = 0$. From the definition of the standard L^2 projection P_h, we have $((\xi_u)_x, \eta_p) = 0$. Then, we take $\theta = \xi_u$ in (A.1), we obtain

$$(\mu(c)k^{-1}\xi_u, \xi_u) = -(\mu(c)k^{-1}\eta_u, \xi_u) - ((\mu(c) - \mu(c_h))k^{-1}u_h, \xi_u). \tag{A.9}$$

Using Cauchy-Schwartz together with the interpolation estimate, we obtain

$$\frac{\mu_*}{k^*}\|\xi_u\|^2 \leq K\|\eta_u\|^2 + \epsilon\|\xi_u\|^2 + K\|c - c_h\|^2, \tag{A.10}$$

where K dependent on $\|u_h\|_\infty$.

Then we have

$$\|u - u_h\| \leq K\|c - c_h\| + Kh^{k+1}. \tag{A.11}$$

Thus we complete the proof of lemma 3.1.

Reference

[1] Arbogast T, Wheeler M F, Yotov I. Mixed finite elements for elliptic problems with tensor coefficients as cell-centered finite differences. SIAM J Numer Anal, 1997, 34: 828-852

[2] Douglas J Jr, Roberts J E. Global Estimates for Mixed Methods for Second Order Elliptic Equations. Math Comp, 1985, 44: 39-52

[3] Douglas J Jr, Ewing R E, Wheeler M F. The approximation of the pressure by a mixed method in the simulation of miscible displacement. RAIRO Numer Anal, 1983, 17: 17-33

[4] Douglas J Jr, Ewing R E, Wheeler M F. A time-discretization procedure for a mixed finite element approximation of miscible displacement in porous media. RAIRO Numer Anal, 1983, 17: 249-265

[5] Reed W H, Hill T R. Triangular Mesh Method for the Neutron Transport Equation. Technical report LA-UR-73-479, Los Alamos Scientific Laboratory, Los Alamos, NM, 1973

[6] Cockburn B, Hou S, Shu C W. The RungeCKutta local projection discontinuous Galerkin finite element method for conservation laws. IV: The multidimensional case. Math Comp, 1990, 54: 545-581.

[7] Cockburn B, Lin S Y, Shu C W. TVB Runge-Kutta local projection discontinuous Galerkin finite element method for conservation laws. III: One-dimensional systems. J Comput Phys, 1989, 84: 90-113

[8] Cockburn B, Shu C W. TVB Runge-Kutta local projection discontinuous Galerkin finite element method for conservation laws. II: General framework. Math Comp, 1989, 52: 411-435

[9] Cockburn B, Shu C W. The Runge-Kutta discontinuous Galerkin method for conservation laws. V: Multidimensional systems. J Comput Phys, 1998, 141: 199-224

[10] Cockburn B, Shu C W. The local discontinuous Galerkin method for time-dependent convection-diffusion systems. SIAM J Numer Anal, 1998, 35: 2440-2463

[11] Bassi F, Rebay S. A high-order accurate discontinuous finite element method for the numerical solution of the compressible Navier-Stokes equations. J Comput Phys, 1997, 131: 267-279.

[12] Yan J, Shu C W. A local discontinuous Galerkin method for KdV type equations. SIAM J Numer Anal, 2002, 40: 769-791

[13] Xu Y, Shu C W. Local discontinuous Galerkin methods for nonlinear Schrodinger equations. J Comput Phys, 2005, 205: 72-97

[14] Xu Y, Shu C W. Local discontinuous Galerkin methods for the KuramotoCSivashinsky equations and the Ito-type coupled KdV equations. Comput Method Appl Mech Eng, 2006, 195: 3430-3447

[15] Castillo P, Cockburn B, Perugia I, Schö tzau D. An a priori error analysis of the local discontinuous Galerkin method for elliptic problems. SIAM J Numer Anal, 2000, 38: 676-706

[16] Castillo P, Cockburn B, Schötzau D, Schwab C. Optimal a priori error estimates for the hp-version of the LDG method for convection diffusion problems. Math Comp, 2002, 71: 455-478

[17] Liu Y X, Shu C W. Error analysis of the semi-discrete local discontinuous Galerkin method for semiconductor device simulation models. Science China Mathematics, 2010, 53 (12): 3255-3278.

[18] Xu Y, Shu C W. Optimal error estimates of the semi-discrete local discontinuous Galerkin methods for high order wave equations. SIAM J Numer Anal, 2012, 50 (1): 79-104

[19] Zhang Q, Gao F Z. A fully-discrete local discontinuous Galerkin method for convection-dominated Sobolev equation. Journal of Scientific Computing, 2012, 51(1): 107-134

[20] Sun S Y, Rivire B, Wheeler M F. A combined mixed finite element and discontinuous Galerkin method for miscible displacement problem in porous media, in: Tony Chan et al. (Eds.), Recent Progress in Computational and Applied PDEs, Kluwer Academic Publishers, Plenum Press, Dordrecht, NewYork, 2002, 323-351

[21] Sun S Y, Wheeler M F. Discontinuous Galerkin methods for coupled flow and reactive transport problems. Appl Numer Math, 2005, 52: 273-298

[22] Arnold D N, Brezzi F, Cockburn B, Marini L D. Unified analysis of discontinuous Galerkin methods for elliptic problems. SIAM J Numer Anal, 2002, 39: 1749-1779

[23] Ciarlet P. The finite element method for elliptic problem, North Holland, 1975.

[24] Bear J. Dynamics of Fluids in Porous Media. Dover Publications, Inc, New York, 1972, 764

[25] Dullien, F. A. L. Porous media fluid transport and pore structure, Academic press, Inc, New York, 1979

[26] Shu C W, Osher S. Efficient implementation of essentially non-oscillatory shock-capturing schemes. J Comput Phys, 1988, 77: 439-471

[27] Douglas J Jr, Roberts J E. Numerical methods for a model for compressible miscible displacement in porous media. Math Comp, 1983, 41: 441-459.

[28] Ayuso B, Carrillo J A, Shu C W. Discontinuous Galerkin methods for the one-dimensional Vlasov-Poisson system. Kinetic and Related Models, 2011, 4: 955-989